DOI: 10.1002/ejic.200700475

Speciation of Uranyl Nitrato Complexes in Acetonitrile and in the Ionic Liquid 1-Butyl-3-methylimidazolium Bis(trifluoromethylsulfonyl)imide

Kelly Servaes,[a] Christoph Hennig,*[b] Isabelle Billard,[c] Clotilde Gaillard,[c] Koen Binnemans,[a] Christiane Görller-Walrand,[a] and Rik Van Deun*[a]

Keywords: EXAFS spectroscopy / Ionic liquids / Uranium / UV/Vis spectroscopy / X-ray absorption spectroscopy

Complex formation between the uranyl ion and nitrate ions in acetonitrile and the ionic liquid 1-butyl-3-methylimidazolium bis(trifluoromethylsulfonyl)imide ($[C_4mim][Tf_2N]$) has been studied by absorption, magnetic circular dichroism (MCD) and uranium L_{III} EXAFS spectroscopy. The experimental results point to the existence of a trinitrate species $[UO_2(NO_3)_3]^-$ with D_{3h} symmetry in both solvents. The atomic distances in the uranium(VI) coordination sphere for the trinitrato complex in acetonitrile are $U–O_{ax}$ = 1.77 ± 0.01 Å and $U–O_{eq}$ = 2.48 ± 0.01 Å. EXAFS data show that the uranyl ion in the ionic liquid is surrounded by six oxygen atoms in the equatorial plane at a distance of 2.49 ± 0.01 Å. The U–N distance of 2.92 ± 0.01 Å indicates a bidentate coordination of the nitrate group in both solvents. A structural comparison is made between the uranyl trinitrato complex anion $[UO_2(NO_3)_3]^-$ and the uranyl tricarbonato complex anion $[UO_2(CO_3)_3]^{4-}$. No evidence is found for the presence of uranyl nitrato complexes in aqueous solution. The optical absorption, MCD and EXAFS spectra resemble those of the hydrated free uranyl ion. There are two axial oxygen atoms at 1.77 ± 0.01 Å and five equatorial oxygen atoms at 2.41 ± 0.01 Å. These values agree well with structural parameters obtained for the uranyl aqua ion.

Introduction

The molecular structure of the uranyl trinitrate complex anion $[UO_2(NO_3)_3]^-$ is well known from X-ray diffraction studies.[1–3] Dieke and Duncan first recorded the absorption spectrum of a $Cs[UO_2(NO_3)_3]$ crystal with a spectrograph and identified the so-called "fluorescent series" and "magnetic series" in the spectrum.[4,5] The magnetic circular dichroism (MCD) spectra of $[UO_2(NO_3)_3]^-$ were first described by Brint and McCaffery[6] and subsequently reinvestigated by Görller-Walrand and Colen,[7] and the electronic transitions and vibrational progressions were first identified by Denning and co-workers by measuring the σ- and π-spectra of $Cs[UO_2(NO_3)_3]$ single crystals.[8] Kaplan and co-workers observed the typical UV/Vis absorption spectrum of the $[UO_2(NO_3)_3]^-$ complex anion in ketone solvents like acetone by adding tetrabutylammonium nitrate to a solution of $UO_2(NO_3)_2$ in these solvents.[9] They noticed a good agreement between the solution spectra and those of $Cs[UO_2(NO_3)_3]$ single crystals. In contrast, these authors could not find a proof for nitrate complex formation in aqueous solution.

Extended X-ray absorption fine structure (EXAFS) spectroscopy measurements on uranyl nitrato compounds are rather scarce, although Thompson and co-workers have investigated the uranyl trinitrato unit in solid $UO_2(NO_3)_2 \cdot 6H_2O$,[10] and the uranyl nitrate dimer in solid $Him_2[\{UO_2(\mu\text{-}OH)(NO_3)_2\}_2]$ (Him = imidazolium) has been studied by Barnes et al.[11] Solvent-extraction processes of uranyl nitrate solutions have been extensively studied because of their significance for nuclear waste treatment.[12–21] These research activities include EXAFS measurements of uranyl nitrate in trimethyl phosphate, tri-*n*-butyl phosphate, triisobutyl phosphate and triphenyl phosphate, which indicate a coordination of two bidentate nitrate groups and two monodentate organophosphate ligands.[20–22] All the experimental EXAFS data obtained to date suffer from competing scattering contributions that cover the important multiple scattering features within the nitrate group. So far, trinitratouranyl species in solution have not been studied in depth by EXAFS spectroscopy, although recently there has been a strong research interest in uranyl complexes, including uranyl nitrate complexes, in ionic liquids.[23–31]

[a] Department of Chemistry, Katholieke Universiteit Leuven, Celestijnenlaan 200F, 3001 Leuven, Belgium
Fax: +32-1632-7992,
E-mail: rik.vandeun@chem.kuleuven.be
[b] Forschungszentrum Dresden-Rossendorf, Institute of Radiochemistry,
P. O. Box 510119, 01314 Dresden, Germany
Fax: +33-476-88-2505,
E-mail: hennig@esrf.fr
[c] Institut Pluridisciplinaire H. Curien, CNRS-IPHC/DRS, Chimie Nucléaire,
B. P. 28, 67037 Strasbourg Cedex 2, France

Supporting information for this article is available on the WWW under http://www.eurjic.org or from the author.

The speciation of uranyl complexes in solution is not always straightforward. Unlike solid-state structures, which can be determined by X-ray diffraction of single crystals, the structure of solution species can be determined only by symmetry effects, for example by optical absorption spectra, or by limited structural parameters obtained, for example, from EXAFS spectra. Various conclusions have been drawn in the past from spectroscopic results, particularly absorption, luminescence and magnetic circular dichroism spectroscopy, and in a previous paper we have demonstrated the existence of a $[UO_2Cl_4]^{2-}$ complex anion with D_{4h} symmetry in acetonitrile by a combination of optical absorption spectroscopy and uranium L_{III} EXAFS spectroscopy.[32] An analogous investigation by the same complementary spectroscopic techniques presented in this paper points to the existence of the uranyl trinitrato complex anion in acetonitrile and the ionic liquid 1-butyl-3-methylimidazolium bis(trifluoromethylsulfonyl)imide ([C_4mim][Tf_2N]). Furthermore, both spectroscopic techniques provide evidence for the absence of a significant degree of complex formation between the uranyl ion and nitrate ions in aqueous solution.

Results and Discussion

The UV/Vis absorption spectrum and the MCD spectrum of uranyl nitrate in the presence of tetrabutylammonium nitrate in acetonitrile are shown in Figure 1. No further changes were observed upon increasing the nitrate concentration above the ratio $[UO_2^{2+}]/[NO_3^-]$ = 1:3, which points to a maximal coordination of the uranyl ion. The most striking feature is the increase in intensity of four bands in the long-wavelength part of the absorption spectrum (21000–24000 cm^{-1}) with respect to the solvated uranyl ion in acetonitrile. These lines correspond to the "magnetic series" reported by Dieke and Duncan for the single-crystal spectra of $Cs[UO_2(NO_3)_3]$, in which the coordination polyhedron of the uranyl ion has a D_{3h} symmetry.[4] The transitions belonging to the magnetic series give rise to very intense, negative A-terms in the MCD spectrum (Figure 1).[7] These MCD signals originate from the electronic transition between the totally symmetric ground state A_1' (Σ_g^+ in $D_{\infty h}$) to the excited state E′ (Δ_g in $D_{\infty h}$).

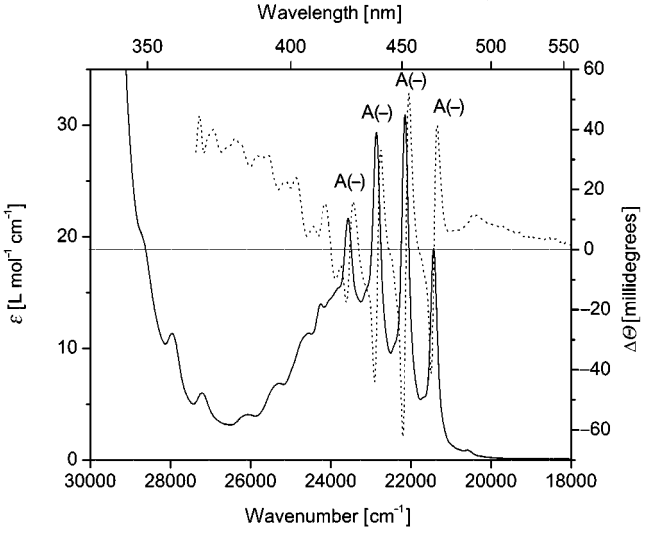

Figure 1. Optical absorption spectrum (solid line) and MCD spectrum (dotted line) of $[UO_2(NO_3)_3]^-$ in acetonitrile at room temperature. $[UO_2^{2+}]$ = 50 and $[NO_3^-]$ = 200 mM ($[UO_2^{2+}]/[NO_3^-]$ = 1:4).

The UV/Vis absorption spectrum and the MCD spectrum of uranyl nitrate in the presence of tetrabutylammonium nitrate in acetone are given as Supporting Information. These spectra are very similar to those recorded in acetonitrile. An overview of all the electronic transitions in the optical absorption spectrum of $[UO_2(NO_3)_3]^-$ in acetonitrile is given in Table 1. A detailed list of the transitions assigned for $[UO_2(NO_3)_3]^-$ in acetonitrile in D_{3h} symmetry is available as Supporting Information. The presence of very intense, sharp peaks in the first part of the optical absorption spectrum is also characteristic of other complexes with D_{3h} trigonal symmetry, such as $[UO_2(CO_3)_3]^{4-}$ and $[UO_2(CH_3COO)_3]^-$.[7,12,33,34]

The optical absorption spectrum and MCD spectrum of $UO_2(NO_3)_2{\cdot}6H_2O$ and Bu_4NNO_3 in the ionic liquid [C_4mim][Tf_2N] are given in Figure 2. The molar absorptivity in this ionic liquid solvent is of the same order of magnitude as that in acetonitrile. The absorption bands can all be assigned to transitions of the uranyl ion since [C_4mim][Tf_2N] does not absorb in this wavelength region.[35] The same typical spectroscopic features of the uranyl trinitrato complex in the range 20000–24000 cm^{-1} (sharp, intense peaks in the optical absorption spectrum

Table 1. Observed electronic transitions for $[UO_2(NO_3)_3]^-$ in acetonitrile and [C_4mim][Tf_2N], assigned to $D_{\infty h}$ and D_{3h} symmetry, compared with those of $Cs[UO_2(NO_3)_3]$ single crystals.[8] Energies are given in wavenumber units [cm^{-1}].

Symmetry		$[UO_2(NO_3)_3]^-$	$[UO_2(NO_3)_3]^-$	$Cs[UO_2(NO_3)_3]$
$D_{\infty h}$	D_{3h}	Acetonitrile	[C_4mim][Tf_2N]	Single crystal[8]
$\Pi_g \leftarrow \Sigma_g^+$	$E'' \leftarrow A_1'$	20585	20563	21090
$\Delta_g \leftarrow \Sigma_g^+$	$E'(x,y) \leftarrow A_1'$	21432	21381	21694
$\Phi_g \leftarrow \Sigma_g^+$	$A_1'' \leftarrow A_1'$	–	–	22300
$(\Delta_g + \Gamma_g) \leftarrow \Sigma_g^+$	$E'(x,y) \leftarrow A_1'$	–	–	23475
$\Phi_g \leftarrow \Sigma_g^+$	$A_1'' \leftarrow A_1'$	–	–	26640
$\Phi_g \leftarrow \Sigma_g^+$	$A_2'' \leftarrow A_1'$	27218	27167	27480

and very intense, negative A-terms in the MCD spectrum) as observed in acetonitrile are also observed in $[C_4mim][Tf_2N]$. Furthermore, the absorption maxima in acetonitrile and $[C_4mim][Tf_2N]$ agree well. The features in the long-wavelength part of the UV/Vis absorption spectrum and the MCD spectrum, as well as a comparison with the well-known $[UO_2(NO_3)_3]^-$ complex in ketone solvents, indicate the formation of a $[UO_2(NO_3)_3]^-$ species in $[C_4mim][Tf_2N]$. The energetic positions of the different electronic states of $[UO_2(NO_3)_3]^-$ in $[C_4mim][Tf_2N]$ are given in Table 1. A detailed assignment of the transitions of $[UO_2(NO_3)_3]^-$ in $[C_4mim][Tf_2N]$ is available as Supporting Information.

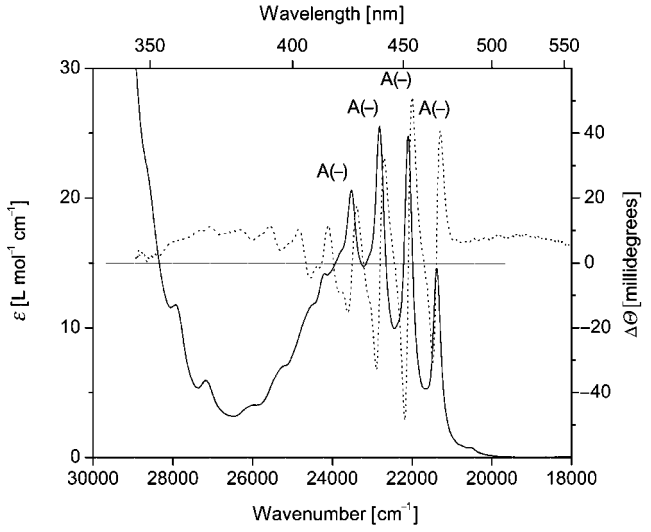

Figure 2. UV/Vis absorption spectrum (solid line) and MCD spectrum (dotted line) of $[UO_2(NO_3)_3]^-$ in $[C_4mim][Tf_2N]$ at room temperature. $[UO_2^{2+}]$ = 50 and $[NO_3^-]$ = 200 mM ($[UO_2^{2+}]/[NO_3^-]$ = 1:4).

An alternative way to obtain the trinitrato complex is to treat UO_2 with concentrated nitric acid in $[C_4mim][Tf_2N]$. However, nitrite ions are also formed in addition to the trinitrato complex, as evidenced by the bands in the region 25000–28500 cm^{-1} in the UV/Vis absorption spectrum (given as Supporting Information). The UV/Vis spectra of nitrite ions and nitrous acid have been described by das Graças Gomes et al.[36] Nevertheless, the presence of the $[UO_2(NO_3)_3]^-$ moiety is also indicated in this case by the intense features in the long-wavelength part of the UV/Vis spectrum.

Spectroscopic measurements indicate that there is no significant complex formation between the uranyl ion and nitrate ions in aqueous solution. The optical absorption spectrum and the MCD spectrum of uranyl nitrate in water exhibit the same vibrational fine structure as that of the free uranyl ion (i.e. the hydrated uranyl ion) obtained by dissolving $UO_2(ClO_4)_2{\cdot}xH_2O$ in water (Figure 3). Moreover, no red- or blueshift of the absorption bands is observed. This similarity between the two spectra suggests that the hydrated uranyl ion is the dominant species in aqueous solution. The absorption spectra of uranyl nitrate $UO_2(NO_3)_2{\cdot}6H_2O$ in aqueous solution can be found in the Supporting Information. The typical sharp absorption bands of the uranyl trinitrato complex are absent in aqueous solution because nitrate ions form only weak complexes in this medium. The system can be characterized by three formation constants: K_1 = 0.5, K_2 = 1.0 and K_3 = 0.9 $L\,mol^{-1}$.[12,37] The formation constants K_1 and K_2 were determined in $NaClO_4$ medium at an ionic strength of 1.0 and K_3 in media of varying HNO_3 concentrations. The species distribution in an aqueous solution of $UO_2(NO_3)_2{\cdot}6H_2O$ (50 mM, pH = 2.4) is dominated by the uranyl aqua ion and the distribution coefficient of the nitrato species is low [94.8% UO_2^{2+}, 4.6% $UO_2NO_3^+$, 0.45% $UO_2(NO_3)_2$ and 0.04% $UO_2(NO_3)_3^-$]. The low-concentration nitrato species cannot be clearly distinguished by UV/Vis absorption spectroscopy. In a recent paper, Ruas and co-workers stated that the equilibrium constants for the 1:1 and 1:2 UO_2^{2+}/NO_3^- complexes are low, which means that the uranyl trinitrato complex in water can be neglected in our case.[38]

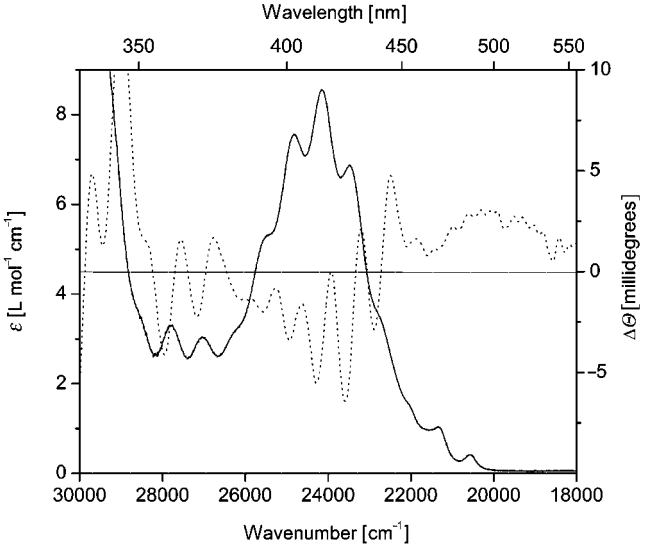

Figure 3. UV/Vis absorption spectrum (solid line) and MCD spectrum (dotted line) of $UO_2(NO_3)_2{\cdot}6H_2O$ in aqueous solution at room temperature. Uranyl concentration: 50 mM.

The UV/Vis absorption spectrum of the hydrated uranyl ion is well known,[5] although the coordination sphere of the hydrated free uranyl ion has always been a point of discussion. Models with four to six water molecules in the equatorial plane have been proposed,[39,40] although it is generally accepted that the uranyl ion is coordinated by five water molecules in the equatorial plane.[41–45]

EXAFS measurements of uranyl nitrate in the presence of tetrabutylammonium nitrate in acetonitrile as well as in $[C_4mim][Tf_2N]$ were performed to confirm the formation of a $[UO_2(NO_3)_3]^-$ species indicated by optical absorption spectroscopy. Furthermore, EXAFS can provide extra structural information, such as bond lengths, for the metal species in solution. Both the EXAFS spectra and corresponding Fourier transforms in acetonitrile and $[C_4mim][Tf_2N]$ exhibit the same structural features (Figure 4). Peaks in the Fourier transforms were not corrected

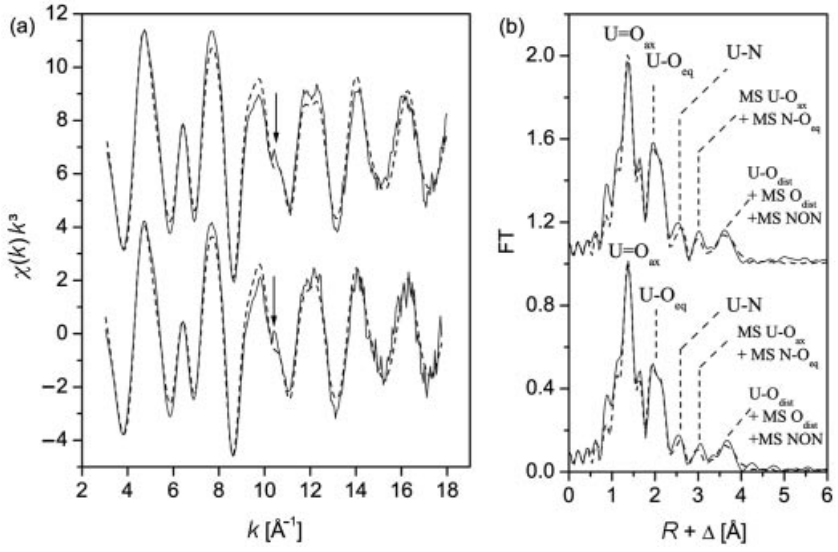

Figure 4. (a) Uranium L_{III}-edge k^3-weighted EXAFS data and (b) the corresponding Fourier transforms of $[UO_2(NO_3)_3]^-$ in acetonitrile (top) and in the ionic liquid $[C_4mim][Tf_2N]$ (bottom). Experimental data are presented as a continuous line and the theoretical curve as a dotted line. The multiple scattering path N–O_{eq}–N is abbreviated as MS NON. The arrow indicates a [2p4f] double-electron excitation.[57]

for the phase shift. The results of the shell-fitting procedure, including phase correction, are given in Tables 2 and 3. The coordination numbers of the equatorial oxygen atoms (O_{eq}) and nitrogen atoms were determined in an iterative manner by a free fit. These coordination numbers were subsequently fixed during the shell-fitting procedure in order to avoid correlation problems between N and σ^2. The coordination number of the distal oxygen atoms was set equal to the coordination number of the nitrogen atoms. The fit results also indicate that three nitrate groups coordinate to uranium(VI) in a bidentate fashion, as shown in Figure 5. The U–O_{eq} distance of 2.48–2.49 Å confirms the sixfold coordination of the uranyl ion as a U–O_{eq} distance between 2.44 and 2.54 Å corresponds to a coordination number of six.[46] The weak peak due to nitrogen backscattering indicates a U–N distance of 2.94 Å (Figure 4). This U–N distance indicates a bidentate coordination of the NO_3^- group and is in good agreement with the U–N distance in solid $Rb[UO_2(NO_3)_3]$ (2.88 Å).[3] The three coordinated nitrate ligands result in complex backscattering features mainly originating from a linear arrangement of the nitrogen atom and the distal oxygen atoms (O_{dist}) in each of the NO_3^- ligands, with respect to the uranium atom. In this situation the scattering amplitude is greatly enhanced in the forward scattering direction due to focusing of the electron wave on the next neighbour. This effect is therefore called the "focusing effect". This focusing effect makes the distal oxygen atoms (O_{dist}) at a large distance of 4.16 (in acetonitrile) or 4.18 Å (in the ionic liquid $[C_4mim][Tf_2N]$) visible. A similar strong multiple scattering effect has been observed for the tricarbonato species $Ca_2[UO_2(CO_3)_3]$ in aqueous solution.[47] The amplitudes of the multiple scattering paths MS O_{dist} (U–N–O_{dist}) and U–N–O_{dist}–N are much more pronounced than that of the single scattering path U–O_{dist}. It is interesting to note that the U–O_{dist} distance in solution is slightly longer than in the solid {4.09 Å in solid $Rb[UO_2(NO_3)_3]$}.[3] The influence of the effective ligand charge on the bond lengths can be revealed by comparing uranium(VI) coordinated by nitrate and carbonate. The uranyl tricarbonato complex anion $[UO_2(CO_3)_3]^{4-}$ is isostructural with the trinitrato anion $[UO_2(NO_3)_3]^-$.[3,47] The U–O_{eq} distance in the uranyl tricarbonato anion is shorter than that in the uranyl trinitrato anion (2.44 vs. 2.48–2.49 Å). Obviously, there is an influence of the U–O_{eq} electron density on the U–O_{ax} bond length, which results in a longer distance (1.81 Å) for the tricarbonato anion and a shorter one (1.77 Å) for the trinitrato anion.[48] The shorter U–O_{ax} distance for the uranyl trinitrato anion can also be deduced from the ground-state vibrational frequencies. Thus, for the uranyl trinitrato anion the symmetric and asymmetric stretching vibrations are 884 and 956 cm^{-1}, respectively, compared to 808 and 856 cm^{-1}, respectively, for the tricarbonato anion. According to Badger's rule,[49,50] the U–O_{ax} distance should therefore be smaller in the uranyl trinitrato anion.

Table 2. EXAFS structural parameters for $[UO_2(NO_3)_3]^-$ in acetonitrile.

	R[a] [Å]	N[a]	σ^2 [Å^2]
U–O_{ax}	1.77	2[b]	0.0012
MS U–O_{ax}	3.54	2[b]	0.0024
U–O_{eq}	2.48	6.4[b]	0.0069
U–N	2.92	3.1[b]	0.0032
MS N–O_{eq}	3.29	12.7[b]	0.0031
U–O_{dist}	4.16	3.1[b]	0.0061
MS O_{dist}	4.16	6.2[b]	0.0061
MS N–O_{dist}–N	4.16	3.1[b]	0.0061

[a] Errors in distances, R, are ±0.01 Å; errors in coordination numbers, N, are ±10%. [b] Value fixed during the shell-fitting procedure. ΔE = 3.85 eV. Weighted F-factor = 0.205.

Table 3. EXAFS structural parameters for $[UO_2(NO_3)_3]^-$ in $[C_4mim][Tf_2N]$.

	R[a] [Å]	N[a]	σ^2 [Å^2]
U–O_{ax}	1.77	2[b]	0.0012
MS U–O_{ax}	3.54	2[b]	0.0024
U–O_{eq}	2.49	6.1[b]	0.0076
U–N	2.92	2.8[b]	0.0036
MS N–O_{eq}	3.28	12.2[b]	0.0054
U–O_{dist}	4.18	2.8[b]	0.0062
MS O_{dist}	4.18	5.6[b]	0.0062
MS N–O_{dist}–N	4.18	2.8[b]	0.0062

[a] Errors in distances, R, are ±0.01 Å; errors in coordination numbers, N, are ±10%. [b] Value fixed during the shell-fitting procedure. ΔE = 3.85 eV. Weighted F-factor = 0.205.

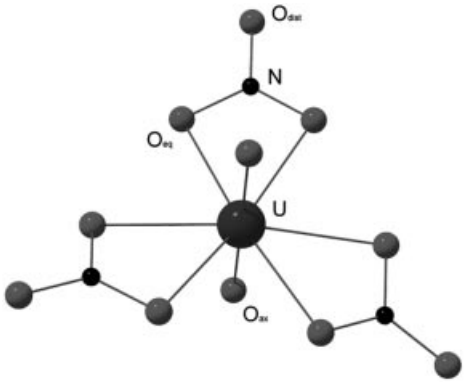

Figure 5. Ball-and-stick representation of the structure of $[UO_2(NO_3)_3]^-$.

The raw k^3-weighted EXAFS data of uranyl nitrate in water are shown in Figure 6. Like the optical absorption spectra, the EXAFS spectra of the aqueous solution show only the typical scattering features of the dominant hydrated uranyl ion. The largest peak in the Fourier transform represents the scattering contribution from the two axial oxygen (O_{ax}) atoms. The double peak at $R + \Delta$ = 1.8 Å arises from one single shell of equatorial oxygen (O_{eq}) atoms. This peak can be completely covered by including one single shell of equatorial oxygen atoms at 2.42 Å in the fitting procedure. The splitting of the O_{eq} shell arises from a superposition of the O_{ax} peak and the O_{eq} peak. Due to the limited k-range, the Fourier transform peaks include small satellite peaks. The rather large satellite peak at high R-values of the O_{ax} peak coincides with the O_{eq} peak, which gives rise to this peak splitting.[51] Peaks in the Fourier transform were not corrected for the phase shift. The structural parameters of the EXAFS shell fitting, including phase correction, are summarized in Table 4. There are two axial oxygen atoms at 1.77 ± 0.01 Å and five equatorial oxygen atoms at 2.41 ± 0.01 Å. A fivefold coordination of the uranyl ion is characterized by a U–O_{eq} distance between 2.34 and 2.42 Å.[46] These values agree well with the structural parameters obtained previously for the uranyl aqua ion in perchloric acid solution.[41,42]

Table 4. EXAFS structural parameters for uranyl nitrate in aqueous solution.

	R[a] [Å]	N[a]	σ^2 [Å^2]
U–O_{ax}	1.77	2[b]	0.0013
MS U–O_{ax}	3.54	2[b]	0.0026
U–O_{eq}	2.41	4.9	0.0069

[a] Errors in distances, R, are ±0.01 Å; errors in coordination numbers, N, are ±10%. [b] Value fixed during the shell-fitting procedure. ΔE = 3.2 eV. Weighted F-factor = 0.273.

Conclusions

We have shown that both UV/Vis absorption and EXAFS spectroscopy point unambiguously to the existence of a $[UO_2(NO_3)_3]^-$ coordination polyhedron (D_{3h} sym-

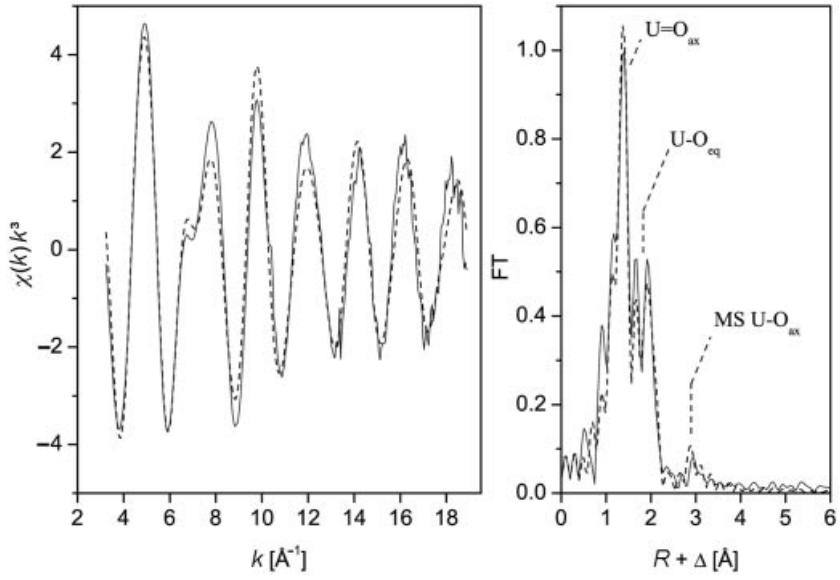

Figure 6. Uranium L_{III}-edge k^3-weighted EXAFS data (left) and the corresponding Fourier transform (right) of uranyl nitrate in aqueous solution. Experimental data are presented as a continuous line and the theoretical curve as a dotted line.

metry) for the uranyl nitrate complex in acetonitrile as well as in the ionic liquid [C_4mim][Tf_2N]. The sharp peaks in the long-wavelength part of the UV/Vis absorption spectra (21000–24000 cm^{-1}) are characteristic of a trigonal symmetry. The fit results of the EXAFS spectra and the corresponding Fourier transforms reveal the presence of six equatorial oxygen (O_{eq}) atoms with U–O bond lengths of 2.48–2.49 Å. The U–N distance of 2.92–2.93 Å points to a bidentate coordination of the NO_3^- group. Furthermore, the distances in the equatorial plane around the uranyl ion for solution species are in good agreement with the distances in solid Rb[$UO_2(NO_3)_3$]. Only the U–O_{dist} distance is slightly longer in solution. The increase in the coordination number from $N_{O_{eq}}$ = 5 (aqua ion) to $N_{O_{eq}}$ = 6 ([$UO_2(NO_3)_3]^-$) involves an increase of the U–O_{eq} bond length from 2.41 to 2.48–2.49 Å. In contrast, no evidence has been found for the presence of uranyl nitrato species in aqueous solution under the given experimental conditions.

Experimental Section

Samples: $UO_2(NO_3)_2{\cdot}6H_2O$ and tetrabutylammonium nitrate (Bu_4NNO_3) were purchased from Merck and Fluka, respectively. Dry acetonitrile was purchased from Acros. An aqueous solution of uranyl nitrate (50 mM) was prepared by dissolving $UO_2(NO_3)_2{\cdot}6H_2O$ in distilled water. The pH of this solution was 2.4. Acetonitrile was used as solvent for measurements in non-aqueous solution instead of acetone because acetonitrile is more stable than acetone in the presence of uranyl ions. Tetrabutylammonium nitrate (Bu_4NNO_3) was added to a solution of $UO_2(NO_3)_2{\cdot}6H_2O$ (50 mM) in acetonitrile to give uranyl/nitrate ratios of beween 1:2 and 1:4. No further changes were observed in the optical absorption spectra at [UO_2^{2+}]/[NO_3^-] ratios higher than 1:3. To obtain the spectrum of the solvated uranyl ion ("free" or "bare" uranyl ion) in acetonitrile, a solution of $UO_2(ClO_4)_2{\cdot}xH_2O$ (50 mM) was prepared as described in ref.[32] 1-Butyl-3-methylimidazolium bis(trifluoromethylsulfonyl)imide ([C_4mim][Tf_2N]) was synthesized as described in ref.[35] To reduce the water content, [C_4mim][Tf_2N] was dried in vacuo at 70 °C before preparing the solutions. $UO_2(NO_3)_2{\cdot}6H_2O$ (50 mM) and tetrabutylammonium nitrate (Bu_4NNO_3; 100 mM) were dissolved in [C_4mim][Tf_2N] to give a total uranyl/nitrate ratio of 1:4. The dissolution of $UO_2(NO_3)_2{\cdot}6H_2O$ and Bu_4NNO_3 in [C_4mim][Tf_2N] took about 3 d and resulted in a transparent, yellow solution. Initial spectroscopic measurements on mixtures of $UO_2(NO_3)_2{\cdot}6H_2O$ and Bu_4NNO_3 in [C_4mim][Tf_2N] did not give the typical absorption spectrum of the uranyl trinitrato complex. However, the [$UO_2(NO_3)_3]^-$ absorption bands were clearly visible when these mixtures were remeasured after several days. This indicates that the kinetics of the formation of the trinitrato complex in the ionic liquid are slow.

Optical Spectroscopy: UV/Vis absorption spectra in aqueous solution, acetonitrile and [C_4mim][Tf_2N] were recorded at room temperature with a Varian Cary 5000 spectrophotometer in the wavelength interval 600–300 nm. Magnetic circular dichroism (MCD) spectra were recorded with an AVIV 62DS circular dichroism spectrometer equipped with an electromagnet (magnetic field strength: 0.9 T) to provide the longitudinal magnetic field.

EXAFS Spectroscopy: Uranium L_{III}-edge EXAFS spectra were collected at the Rossendorf Beamline at the European Synchrotron Radiation Facility (ESRF, Grenoble, France).[52] The measurements were carried out in transmittance mode using argon-filled ionization chambers at ambient temperature and pressure. Higher harmonics were rejected with two platinum-coated mirrors. The measurements were performed using a double-crystal Si(111) monochromator in equidistant k-steps of 0.05 $Å^{-1}$ across the EXAFS region. Three scans were recorded for each sample and then averaged. An yttrium metal foil (first inflection point at 17038 eV) was used for energy calibration. The uranium L_{III} threshold energy, $E_{k=0}$, was defined at 17185 eV. EXAFS data were extracted from the raw absorption spectra by standard methods, including a spline approximation for the atomic background with the program EXAFSPAK.[53] Theoretical phase and amplitude functions were calculated with FEFF 8.2.[54] The scattering phase and amplitude functions were calculated using the crystal structure of uranyl dinitrate trihydrate, $[UO_2(NO_3)_2(H_2O)_2]{\cdot}H_2O$,[55] and the rubidium uranyl salt Rb[$UO_2(NO_3)_3$].[3] The amplitude reduction factor, S_0^2, was found to be 0.9 from the FEFF calculation and fixed to that value in the data fits. The coordination number of the uranyl oxygen atoms (O_{ax}) in all fits was kept constant at two. The main multiple scattering paths, with their relative importance, are defined according to the notation in Figure 5 and given in the Supporting Information. Hudson and co-workers have indicated that the scattering contributions from paths U–O_{ax1}–O_{ax2} and U–O_{ax1}–U–O_{ax1} tend to cancel each other out,[56] therefore the twofold-degenerate, four-legged multiple scattering path U–O_{ax1}–U–O_{ax2} (abbreviated as MS U–O_{ax}) was included in the curve fit by constraining its Debye–Waller factor, σ^2, and its effective path length to twice the values of the corresponding, freely fitted U–O_{ax} single scattering path. The degeneracy of the multiple scattering paths was included in the coordination numbers N, therefore the degeneracy of the dominating multiple scattering paths including the distal oxygen O_{dist}, namely U–N–O_{dist}–N and U–O_{dist}–N (abbreviated as MS O_{dist}), was fixed to twice the value of the number of distal oxygen atoms present. Furthermore, the distances and Debye–Waller factor for these multiple scattering paths were linked to R and σ^2 of the single scattering path U–O_{dist}. The number of scattering paths of the three-legged multiple scattering path U–N–O_{eq} was constrained to twice the coordination number of the equatorial oxygen atoms O_{eq}, whereas R and σ^2 were kept free in the fit. Scattering contributions of less than 5% were not considered in the fitting procedure.

Supporting Information (see footnote on the first page of this article): Correlation table of the irreducible representations in the different D_{nh} point groups; UV/Vis absorption spectrum and data of $UO_2(NO_3)_2{\cdot}6H_2O$ in water; UV/Vis absorption spectrum and observed vibronic transitions of [$UO_2(NO_3)_3]^-$ in acetonitrile, acetone, and [C_4mim][Tf_2N]; UV/Vis absorption spectrum of UO_2 powder dissolved in [C_4mim][Tf_2N] with the help of HNO_3/H_2O; MCD and UV/Vis absorption spectra of $Bu_4NUO_2(NO_3)_3$ in a PMMA matrix; principal scattering pathways of the photoelectron in the [$UO_2(NO_3)_3]^-$ unit.

Acknowledgments

The EXAFS measurements were performed at the Rossendorf Beamline at the ESRF. K. S. is a research assistant and R. V. D. a postdoctoral fellow of the Fund for Scientific Research, Flanders (Belgium) (FWO-Vlaanderen). This project was financed by the FWO-Vlaanderen (project G.0508.07) and by the K. U. Leuven (projects GOA03/03 and IDO/05/005). R. V. D. acknowledges financial support from the FWO-Vlaanderen ("Krediet aan Navorsers" project 1.5.099.06) and C. H. acknowledges financial support from the DFG (HE 2297/2-1).

[1] S. S. Malcic, L. M. Manojlovic, *Bull. Inst. Nucl. Sci. "Boris Kidrich"*, **1961**, *11*, 135–139.
[2] G. A. Barclay, T. M. Sabine, J. C. Taylor, *Acta Crystallogr.* **1965**, *19*, 205–209.
[3] A. Zalkin, L. K. Templeton, D. H. Templeton, *Acta Crystallogr., Sect. C* **1989**, *45*, 810–811.
[4] G. H. Dieke, A. B. F. Duncan, *Spectroscopic Properties of Uranium Compounds*, McGraw Hill, New York, **1965**.
[5] E. Rabinowitch, R. L. Belford, *Spectroscopy and Photochemistry of Uranyl Compounds*, Pergamon, Oxford, **1964**.
[6] P. Brint, A. J. McCaffery, *Mol. Phys.* **1973**, *25*, 311–322.
[7] C. Görller-Walrand, W. Colen, *Inorg. Chim. Acta* **1984**, *84*, 183–188.
[8] R. G. Denning, D. N. P. Foster, T. R. Snellgrove, D. R. Woodwark, *Mol. Phys.* **1979**, *37*, 1089–1107.
[9] L. Kaplan, R. A. Hildebrandt, M. Ader, *J. Inorg. Nucl. Chem.* **1956**, *2*, 153–163.
[10] H. A. Thompson, G. E. Brown Jr, G. A. Parks, *Am. Min.* **1997**, *82*, 483–496.
[11] C. E. Barnes, Y. Shin, S. Saengkerdsub, S. Dai, *Inorg. Chem.* **2000**, *39*, 862–864.
[12] J. J. Katz, G. T. Seaborg, L. R. Morss, *The Chemistry of the Actinide Elements*, Chapman and Hall, New York, **1986**.
[13] Yu. A. Zolotov, *Macrocyclic Compounds in Analytical Chemistry*, John Wiley & Sons, New York, **1997**.
[14] Yu. S. Fedorov, B. Ya. Zilberman, *Radiochemistry* **2000**, *42*, 242–246.
[15] Yu. S. Fedorov, B. Ya. Zilberman, *Radiochemistry* **1999**, *41*, 545–550.
[16] Yu. S. Fedorov, I. V. Blazheva, B. Ya. Zilberman, *Radiochemistry* **2000**, *42*, 74–78.
[17] Yu. S. Fedorov, B. Ya. Zilberman, S. M. Kulikov, I. V. Blazheva, E. N. Mishin, *Solvent Extr. Ion Exch.* **1999**, *17*, 243–257.
[18] Y. Oda, H. Funasaka, Y. Nakamura, H. Adachi, *J. Alloys Compd.* **1997**, *255*, 24–30.
[19] A. K. Mohammed, J. C. Sullivan, K. L. Nash, *Solvent Extr. Ion Exch.* **2000**, *18*, 809–820.
[20] C. Den Auwer, C. Lecouteux, M. C. Charbonnel, C. Madic, R. Guillaumont, *Polyhedron* **1997**, *16*, 2233–2238.
[21] C. Den Auwer, M. C. Charbonnel, M. T. Presson, C. Madic, R. Guillaumont, *Polyhedron* **1998**, *17*, 4507–4517.
[22] R. Chiarizia, M. P. Jensen, M. Borkowski, J. R. Ferraro, P. Thiyagarajan, K. C. Littrell, *Solvent Extr. Ion Exch.* **2003**, *21*, 1–27.
[23] K. Binnemans, *Chem. Rev.* **2007**, *107*, 2592–2614.
[24] V. A. Cocalia, K. E. Gutowski, R. D. Rogers, *Coord. Chem. Rev.* **2006**, *250*, 755–764.
[25] P. Giridhar, K. A. Venkatesan, T. G. Srinivasan, P. R. V. Rao, *J. Radioanal. Nucl. Chem.* **2005**, *265*, 31–38.
[26] M. O. Sornein, C. Cannes, C. Le Naour, G. Lagarde, E. Simoni, J. C. Berthet, *Inorg. Chem.* **2006**, *45*, 10419–10421.
[27] A. E. Bradley, C. Hardacre, M. Nieuwenhuyzen, W. R. Pitner, D. Sanders, K. R. Seddon, R. C. Thied, *Inorg. Chem.* **2004**, *43*, 2503–2514.
[28] A. Chaumont, G. Wipff, *Inorg. Chem.* **2004**, *43*, 5891–5901.
[29] C. Gaillard, A. El Azzi, I. Billard, H. Bolvin, C. Hennig, *Inorg. Chem.* **2005**, *44*, 852–861.
[30] A. E. Visser, M. P. Jensen, I. Laszak, K. L. Nash, G. R. Choppin, R. D. Rogers, *Inorg. Chem.* **2003**, *42*, 2197–2199.
[31] C. Gaillard, A. Chaumont, I. Billard, C. Hennig, A. Ouadi, G. Wipff, *Inorg. Chem.* **2007**, *46*, 4815–4826.
[32] K. Servaes, C. Hennig, R. Van Deun, C. Görller-Walrand, *Inorg. Chem.* **2005**, *44*, 7705–7707.
[33] C. Görller-Walrand, S. De Jaegere, *J. Chim. Phys.* **1972**, *4*, 726–736.
[34] S. De Houwer, C. Görller-Walrand, *J. Alloys Compd.* **2001**, *323–324*, 683–687.
[35] P. Nockemann, K. Binnemans, K. Driesen, *Chem. Phys. Lett.* **2005**, *415*, 131–136.
[36] M. das Graças Gomes, S. da S. S. Borges, L. G. F. Lopes, D. W. Franco, *Anal. Chim. Acta* **1993**, *282*, 81–85.
[37] *Gmelin Handbook*, U, Uranium suppl. vol. D1 ("Properties of uranium ions in solutions and melts"), system number 55, Springer, Berlin, **1984**.
[38] A. Ruas, O. Bernard, B. Caniffi, J.-P. Simonin, P. Turq, L. Blum, P. Moisy, *J. Phys. Chem. B* **2006**, *110*, 3435–3443.
[39] J.-C. G. Bünzli, *J. Alloys Compd.* **1993**, *192*, 266–270.
[40] S. Spencer, L. Gagliardi, N. C. Handy, A. G. Ioannou, C.-K. Skylaris, A. Willetts, A. M. Simper, *J. Phys. Chem. A* **1999**, *103*, 1831–1837.
[41] V. Vallet, U. Wahlgren, B. Schimmelpfennig, H. Moll, Z. Szabó, I. Grenthe, *Inorg. Chem.* **2001**, *40*, 3516–3525.
[42] C. Hennig, J. Tutschku, A. Rossberg, G. Bernhard, A. C. Scheinost, *Inorg. Chem.* **2005**, *44*, 6655–6661.
[43] M. Bühl, R. Diss, G. Wipff, *J. Am. Chem. Soc.* **2005**, *127*, 13506–13507.
[44] J. Neuefeind, L. Soderholm, S. Skanthakumar, *J. Phys. Chem. A* **2004**, *108*, 2733–2739.
[45] C. Görller-Walrand, W. Colen, *Chem. Phys. Lett.* **1982**, *93*, 82–85.
[46] M. R. Antonio, L. Soderholm, *The Chemistry of the Actinide and Transactinide Elements*, Springer, Dordrecht, The Netherlands, **2006**, vol. 5, pp. 3086–3198.
[47] G. Bernhard, G. Geipel, T. Reich, V. Brendler, S. Amayri, H. Nitsche, *Radiochim. Acta* **2001**, *89*, 511–518.
[48] S. P. McGlynn, J. K. Smith, W. C. Neely, *J. Chem. Phys.* **1961**, *35*, 105–116.
[49] R. G. Denning, *Struct. Bonding (Berlin)* **1992**, *79*, 215–276.
[50] J. R. Bartlett, R. P. Cooney, *J. Mol. Struct.* **1989**, *193*, 295–300.
[51] C. Hennig, K. Schmeide, V. Brendler, H. Moll, S. Tsushima, A. C. Scheinost, *Inorg. Chem.*; DOI: 10.1021/ic0619759.
[52] W. Matz, N. Schell, G. Bernhard, F. Prokert, T. Reich, J. Claußner, W. Oehme, R. Schlenk, S. Dienel, H. Funke, F. Eichhorn, M. Betzl, D. Pröhl, U. Strauch, G. Hüttig, H. Krug, W. Neumann, V. Brendler, P. Reichel, M. A. Denecke, H. Nitsche, *J. Synchrotron Radiat.* **1999**, *6*, 1076–1085.
[53] G. N. George, I. J. Pickering, *EXAFSPAK, a suite of computer programs for analysis of X-ray absorption spectra*, Stanford Synchrotron Radiation Laboratory, Stanford, **2000**.
[54] A. L. Ankudinov, B. Ravel, J. J. Rehr, S. D. Conradson, *Phys. Rev. B* **1998**, *58*, 7565–7576.
[55] R. R. Shuvalov, P. C. Burns, *Acta Crystallogr., Sect. C* **2003**, *59*, i71–i73.
[56] E. A. Hudson, P. G. Allen, L. J. Terminello, M. A. Denecke, T. Reich, *Phys. Rev. B* **1996**, *54*, 156–165.
[57] C. Hennig, *Phys. Rev. B* **2007**, *75*, 035120-1-7.

Received: May 2, 2007
Published Online: September 18, 2007

